Heterogeneous Base-Catalyzed Conversion of Glycolaldehyde to Aldotetroses

Mechanistic and Kinetic Insight

Barsøe, Linette Rønn; Saravanamurugan, Shunmugavel; Taarning, Esben; Espin, Juan Salvador Martinez; Meier, Sebastian

Published in:
ChemCatChem

Link to article, DOI:
10.1002/cctc.202101347

Publication date:
2021

Document Version
Peer reviewed version

ChemCatChem

The European Society Journal for Catalysis

Chemistry Europe

European Chemical Societies Publishing

Supported by GECATS GERMAN CATALYSIS SOCIETY

Accepted Article

Title: Heterogeneous Base-Catalyzed Conversion of Glycolaldehyde to Aldotetroses: Mechanistic and Kinetic Insight

Authors: Linette Rønn Barsøe, Shunmugavel Saravanamurugan, Esben Taarning, Juan Salvador Martinez Espin, and Sebastian Meier

To be cited as: *ChemCatChem* 10.1002/cctc.202101347

Link to VoR: https://doi.org/10.1002/cctc.202101347

WILEY-VCH

FULL PAPER WILEY-VCH

Heterogeneous Base-Catalyzed Conversion of Glycolaldehyde to Aldotetroses: Mechanistic and Kinetic Insight

Linette Rønn Barsøe,[a,b] Shunmugavel Saravanamurugan,[c] Esben Taarning,[a] Juan Salvador Martinez Espin,[a]* and Sebastian Meier[b]*

[a] L. R. Barsøe, Dr. E. Taarning, Dr. J.S.M. Espin
New Business R&D Haldor Topsøe A/S
Haldor Topsøes Allé 1,
2800-Kgs. Lyngby (Denmark)
E-mail: JSME@topsoe.com

[b] L. R. Barsøe, Dr. S. Meier
Department of Chemistry
Technical University of Denmark
Kemitorvet, 2800-Kgs. Lyngby (Denmark)
E-mail: semei@kemi.dtu.dk

[c] Dr. S. Saravanamurugan
Laboratory of Bioproduct Chemistry,
Center of Innovative and Applied Bioprocessing, 140306 Mohali (India)

Supporting information for this article is given via a link at the end of the document.

Abstract: Recent strides towards greater sustainability in materials and energy production have led to a resurgence in the study and utilisation of carbohydrates. Opposite to C6 and C5 carbohydrates, C4 carbohydrates (tetroses) are much less accessible from biological sources. A promising approach for the production of C4 carbohydrates is the cracking of C6 carbohydrates to C2 fragments, and the subsequent combination of two C2 fragments to tetroses. Here, we show that the suitable choice of reaction conditions can kinetically stabilize the rare aldotetroses threose (THR) and erythrose (ERY). The latter approach yields THR and ERY at high selectivity under benign conditions, using commercial resins with tertiary amine groups as the catalyst. Isotope incorporation into GA in D_2O solvent is introduced as a reference reaction to probe the competitive formation of aldotetroses and deuterated GA from a low-populated, not directly detected enediol intermediate that is formed in the rate-determining step. Reaction progress tracked *in situ* by NMR and *ex situ* by chromatography validates that the overall conversion is of first order with respect to GA due to the slow initial enolization. Cyclization of the aldotetroses slows their further conversion to thermodynamically more stable erythrulose and C6 sugars.

Introduction

Carbohydrates form the majority of renewable biomass on earth and can be obtained in pure form as prospective substrates for the production of hitherto fossil-based or even unavailable chemicals.[1] The majority of naturally occurring carbohydrates are C6 (hexose) or C5 (pentose) carbohydrates. Different carbohydrates are distinctly suited for the use in processes towards different products. Beyond the number of constituent carbon atoms, the propensity of different carbohydrates to enter distinct reaction pathways can be rationalized with their different stereochemistry, energy and propensity to form cyclic or open structures.

Processes for the conversion of carbohydrates involve isomerization, dehydration and the formation or breakage of carbon-carbon bonds.[1-2] Examples include the isomerization of carbohydrates to rare sugars, the dehydration to furanic compounds,[2b, 2e] or the conversion to polymer building blocks.[3] Increasingly, attention has been devoted to the prospect of building bio-sourced molecules up from the smallest possible carbohydrates such as the C2 aldose glycolaldehyde (GA).[2c, 4] GA can be derived by thermal conversions of glucose and other carbohydrates and such processes are currently being developed, including pyrolysis, gasification, catalytic retroaldol cleavage, use of supercritical water or thermal cracking in yields of up to 74%.[4b, 5] GA itself emerges as a precursor for polymer or pharmaceuticals production upon conversion to other C2 compounds such as ethylene glycol, ethanolamine, glyoxal, glycolic acid, or glyoxylic acid.[2f, 4b]

Alternatively, GA can be used to build carbon chains, when using the aldehyde functionality for aldol additions. Aldol addition is an appealing approach not only for extending the carbon chain length, but also for attaining quantitative atom economy, as no byproduct forms during the reaction. Aldol addition of GA leads to C4 carbohydrates (tetroses) as intermediates, and subsequently to longer carbohydrates.[2f] Tetroses could form a platform for new bio-sourced compounds, but such activities have been hindered by the high cost of tetroses. Arguably, processes for the formation of bio-sourced C4 compounds have been somewhat neglected due to the scarcity of tetroses in nature. Promising C4 products derived from tetroses include the sweetener erythritol, the polymer building blocks methyl vinyl glycolate and methoxy-2-hydroxy-3-butenoate and the precursor γ-butyrolactone. GA thus is a prospective substrate for the formation of C4 compounds via tetrose intermediates.

The most common catalysts used in aldol addition of GA have included bases,[2a, 6] minerals,[7] amino acids and peptides,[8] as well as homogeneous and heterogeneous Lewis acidic catalysts.[2a, 2c, 9] Conditions that stabilize valuable tetroses in the aldol addition of GA have attracted interest. Thus, shape-selectivity in Lewis acidic zeolites has been exploited to suppress the continued aldol addition of tetrose intermediates with GA to hexoses. [2f, 9a] To this end, microporous zeolite catalysts with suitable pore dimensions and mild reaction conditions of below 373 K were used in organic solvents and water. This approach yielded a mixture of the aldotetroses

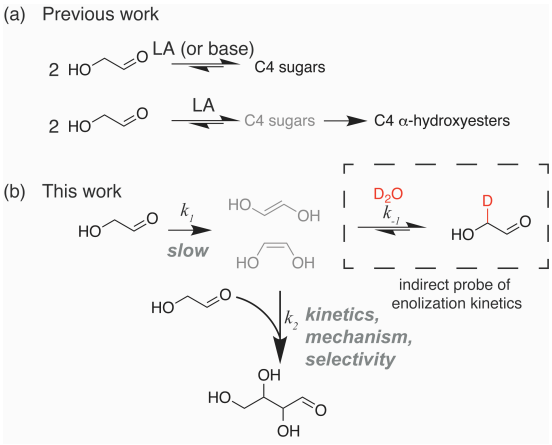

Scheme 1. (a) GA has been described as a promising substrate for the formation of tetroses, especially ERU, and of C4 polymer building blocks that are formed from tetrose intermediates generated *in situ*. (b) The current study investigates the viability and mechanistic basis for the conversion of GA to the rare aldotetroses ERY and THR with cheap reactants and catalysts.

threose (THR) and erythrose (ERY), and predominantly the more stable ketotetrose erythrulose (ERU) with reported yields of up to 74%.[2f, 9a] The [2+2] aldol addition of two GA units to tetroses can also be catalysed by cheap basic resins (such as the weak base resin Amberlyst® A21, containing tertiary amine groups) in water, albeit the stability of the resins and the further reaction of tetroses to few percent of hexoses have remained a concern.[2f, 9a] Beyond the formation of bio-sourced chemicals, the facile aldol reaction of GA to longer sugars under mild conditions has also attracted interest due to its implications for the beginning-of-life chemistry. [7d, 8, 10] Among those studies, Kim et al.[7d] employed minerals as homogeneous base catalysts to convert GA to aldotetroses in yields reaching 86%.

Here, we sought insight into the reaction mechanism and into the prospect for selective production, especially of THR and ERY, with cheap and accessible reagents. We hypothesized that using base- rather than Lewis acid catalysis in conjunction with very mild reaction conditions would kinetically stabilize THR and ERY, thus permitting their selective production. To this end, time-resolved *ex situ* and *in situ* tracking of reaction progress was conducted (Scheme 1).

Results and Discussion

Substrate forms, temperature dependence

The aldol addition of GA under basic conditions involves an enolization to 1,2-ethenediol (possibly in its anionic form) upon α-proton abstraction, which enables the nucleophilic addition of the 1,2-ethenediol to the carbonyl group of another GA molecule.[2a, 11] The equilibrium between GA and 1,2-ethenediol is strongly shifted towards the aldehyde form.[12] In an aqueous solution, GA is further predominantly hydrated at C1. We conducted our studies under concentrations of GA that are relevant for intensification of the process and employed GA at mass fractions above 5%. Under these conditions, GA also forms oligomers in aqueous solution. Hence, the GA substrate forms a complex ensemble of mostly

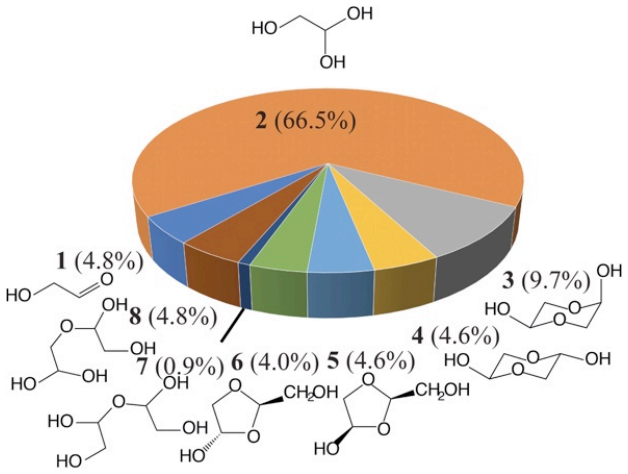

Figure 1. Distribution of main forms of GA at 298 K, 50 mg GA, 450 µl H_2O/50 µl D_2O.

dimeric and monomeric aldehyde and hydrate forms in aqueous solution.[12] ^1H and ^{13}C chemical shift assignments for some of the forms present in the aqueous solution are given in Figure S1. Overall, the minority of GA exists in free monomeric aldehyde form at the outset of the reaction. The equilibrium between the aldehyde and the hydrate forms of GA was characterized by determining the equilibrium distribution at varying temperatures. In this manner, the standard enthalpies and entropies of dehydration were determined, showing that dehydration is endothermic and entropically driven. The experimental equilibrium constant increased from 0.05 to 0.14 between 303 and 333 K, thus showing that the population of the free aldehyde increases rather significantly with temperature, at relevant mild reaction temperatures (Figure S2). The presence of the free aldehyde is required for enolization and for aldol addition. Notably, the population of free aldehyde forms of aldotetroses at 333 K has been determined to be only 3%, due to the ability of aldotetroses (and longer aldoses) to form low-energy rings.[13]

Tracking enolization via isotope exchange

Many mechanisms of carbohydrate conversion (including e.g. ketose-to-aldose interconversion and Lewis-acid catalysed dehydrations) are thought to entail initial enolization steps that activate the carbohydrate for subsequent reactions.[2e, 14] The low population of enol forms complicates the kinetic and mechanistic study of all the emerging processes that convert carbohydrates to bio-sourced substrates. We hypothesized that deuterium isotope incorporation into GA could be used as a reporter reaction that indirectly probes enolization kinetics in D_2O solvent. The vast predominance of GA relative to 1,2-ethenediol implies that the rate constant for GA formation is orders of magnitude larger than the rate constant for the formation of 1,2-ethenediol ($k_1 << k_{-1}$ in Scheme 1). Hence, the deuteration of GA by the commercial basic catalyst Amberlyst® A21 (AA21) was followed and was compared to the kinetics of the [2+2] aldol addition resulting in tetroses. *In situ* ^{13}C NMR spectroscopy was used to compare the emergence of tetroses and the formation of the deuterated isotopic isomer of GA by a time series of one-dimensional ^{13}C NMR spectra (Figure 2).

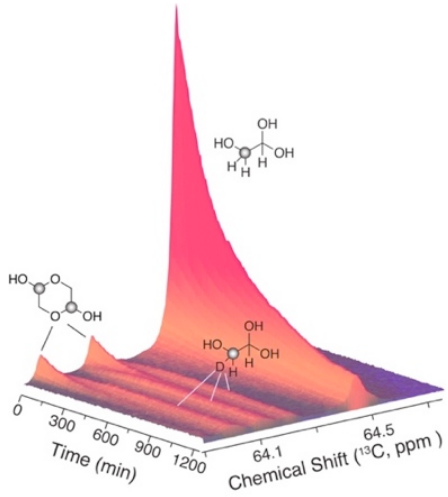

Figure 2. Real-time *in situ* ^{13}C NMR observation of the decay of protonated GA (hydrate form) and emergence of deuterated GA as a reporter of enolization (see also Figure 6a). The deuterated ^{13}C site is split into a triplet by deuterium, as no ^{2}H decoupling was applied for clarity. Reaction conditions: 50 mg GA, 500 µl D_2O, 20 mg AA21, 333 K.

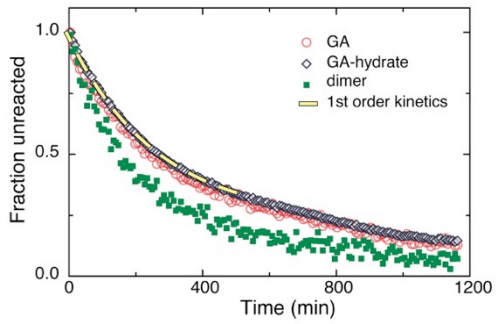

Figure 3. Fraction of unreacted GA, hydrate form and dimer forms over time. Conversion of GA-hydrate is fitted to a first-order kinetics. Reaction conditions: 50 mg GA, 500 µl D_2O, 20 mg AA21, 333 K.

Rate-determining enolization is followed by competing aldol addition or isotope exchange

The kinetics of all forms of GA conversion closely followed an exponential decay with time, thus indicating a rate-determining step that is of first order with respect to GA concentration (Figure 3).[15] The time course of the GA concentration decay resembles the time course for its hydrate form, thus indicating that these forms equilibrate fast relative to reaction progress. Dimer forms decay faster than monomer forms due to the decrease in overall GA concentration over time, leading to a shift towards monomeric forms upon GA conversion (Figure 3 and S3). In the absence of catalyst, the different GA forms remained constant over time (Figure S4). Opposite to the equilibration of GA forms under reaction conditions, deuteration of GA did not occur quickly, but proceeded on the time-scale of hours in parallel to reaction progress Figure 2, 3).

The reaction order was validated by the use of initial rate measurements under varying substrate concentrations. These measurements corroborated that the conversion of GA by AA21 was of first order with respect to the GA concentration (Table S1) at the substrate concentrations of >5% w/v used herein. Box plots for the determination of first- and second-order rate constants under four conditions with varying reactant concentrations are shown in Figure 4 and likewise show that the kinetic results are consistent with a reaction that is of first order with respect to GA concentration.

The first-order kinetics of GA conversion can be rationalized by treating the reaction kinetics with the steady state approximation, entailing that the enol form reacts rapidly upon its formation. Analytical treatment with the steady state approximation yields a rate law for the loss of GA concentration equal to

$$\frac{d[GA]}{dt} = \frac{-2k_1 \cdot k_2 \cdot [GA]^2}{k_2 \cdot [GA] + k_{-1}},$$

with the rate constants k_1, k_{-1} and k_2 as defined in Scheme 1 and a derivation as detailed in the Supporting Information. Hence, the observed first-order reaction rate is consistent with $k_2 \cdot [GA] > k_{-1}$, i.e. fast aldol addition relative to tautomerism for sufficiently high GA concentrations, while the reaction will approach second-order kinetics, if GA concentration is sufficiently low that $k_2 \cdot [GA] < k_{-1}$.

The kinetics of aldotetrose formation is shown in Figures 5 and 6. THR and ERY are the predominant products formed with high selectivity. These tetroses are the expected immediate products of the aldol addition of GA and its enediol form. Approximately three times more THR was formed as compared to ERY, and the THR to ERY ratio was independent of time. This parallel formation of THR and ERY is expected for competitive reactions, where the population of products reflects the rate constant of their formation at any time. Control experiments

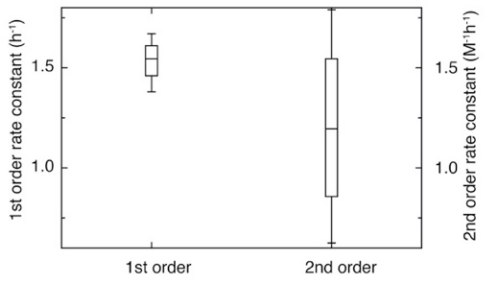

Figure 4. Box plots of the distributions of rate constants derived from four initial rate measurements and assuming first and second order kinetics with respect to GA. Reaction conditions: 100 mL H_2O, GA ranging from 50-200 g/L and AA21 ranging from 10-40 g/L; 313 K. Rates were normalized relative to the number of catalyst active sites as determined by titration.

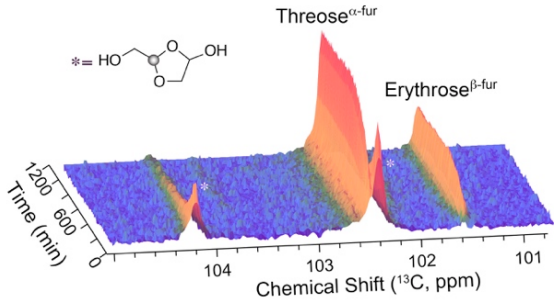

Figure 5. Real-time *in situ* ^{13}C NMR observation of THR and ERY formation. Dimeric GA forms are indicated by an asterisk. Reaction conditions: 50 mg GA, 500 µl D_2O, 20 mg AA21, 333 K.

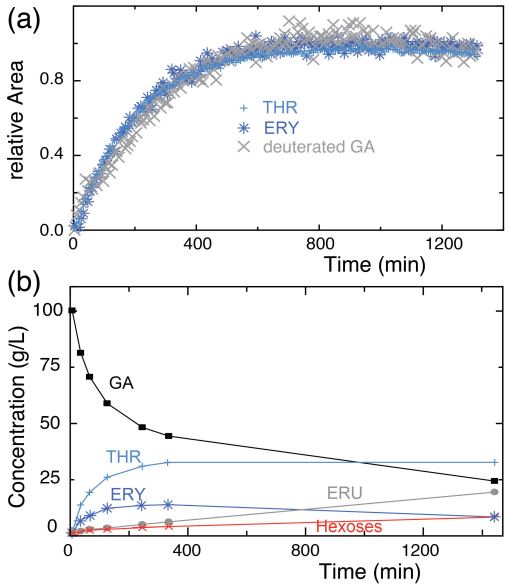

Figure 6. (a) In situ NMR-derived kinetic profiles for the formation of THR, ERY and deuterated GA over time. Reaction conditions: 50 mg GA, 500 µl D_2O, 20 mg AA21, 333 K. (b) Kinetic profiles under stirring in a batch reactor, displaying ERU and hexose formation. Reaction conditions: 10 g GA, 100 mL H_2O, 4 g AA21, 333 K.

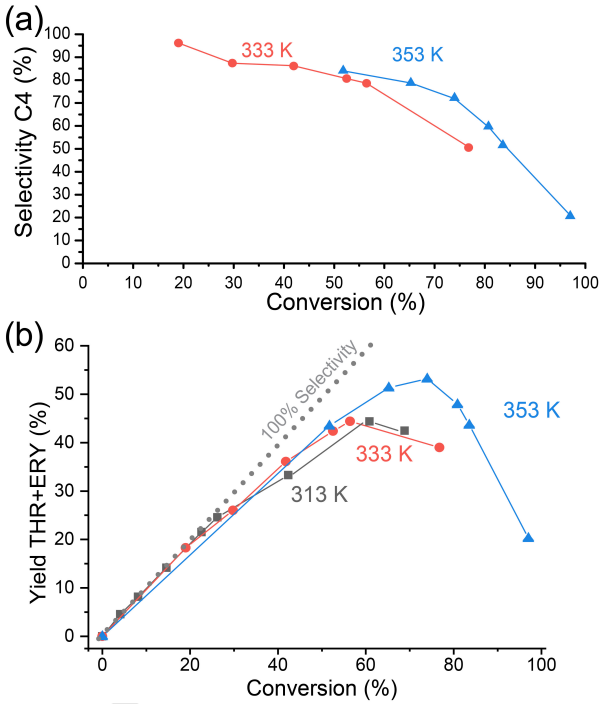

Figure 7. Selectivity in the formation of tetroses (a) and yield of aldotetroses (b) as a function of conversion in a batch reactor, showing higher selectivity and higher maximum yields at higher temperature. Reaction conditions: 10 g GA, 100 mL H_2O, 4 g AA21, and indicated temperature.

showed that the conversion of GA to tetroses was nearly irreversible under the mild temperatures that were employed (<353 K).

Beyond following each other's kinetic profiles, the formation of ERY and THR also followed the same kinetic profile as the incorporation of deuterium from solvent into GA (Figure 6a), which was employed as a reference reaction for GA enolization as detailed above (Figure 2). This reference reaction thus indicates that the formation of deuterated GA, THR and ERY proceed from competing reactions of a low-populated 1,2-ethenediol intermediate, which is formed in a rate-determining first-order reaction step. Reaction rates towards THR and ERY in the aldol addition were comparable to the tautomerization of 1,2-ethenediol to deuterated GA. THR, ERY and (deuterated) GA thus emerged in relative ratios of approximately 3.0:1.0:1.6, when reacting GA in D_2O at 333 K.

Apart from the competing reversible tautomerization of 1,2-ethenediol to GA substrate, the selectivity of the reaction system towards THR and ERY products can be remarkably high. In protonated solvent, conversion of GA to THR and ERY proceeded with a selectivity of approximately 80% at a level of conversion of up to 65% (Table S2). In these reactions, maximum yields above 53% aldotetrose were obtained at 353 K, while maximum yields of aldotetroses were 35% and 46% at 313 K and 333 K, respectively. Maximum yields of aldotetroses were obtained at conversions of 42%, 56% and 74% at reaction temperatures of 313 K, 333 K and 353 K, respectively. A detailed overview of yields and selectivities at various levels of conversion and conditions is given in Figure 7. An analysis of the reaction rates at these temperatures using the Eyring equation of the transition state theory yields enthalpies and entropies of activation of $\Delta H^{\neq} = 70$ kJ/mol and $\Delta S^{\neq} = -86$ J/(mol·K) respectively for the aldol reaction with AA21.

Rationales for kinetic stabilization of aldotetroses

THR and ERY were not the thermodynamic reaction products of GA conversion by AA21, as expected. After extended reaction times (Figure 6b), or in the presence of high loadings of AA21 (Figure S5), ERU and (to a lesser degree) hexoses emerged at the expense of THR and ERY (Figure 7b). The hexoses were previously shown to entail all eight aldohexoses, and ERU and hexoses had previously been described as the thermodynamically more stable products as compared to the aldotetroses (see Figure S5 for a visualization using an excess of basic resin).[2f, 16] Hence, the question arises, why and under which conditions THR and ERY are kinetically stabilized products that react more slowly with the enediol form of GA than GA itself does.

The isomerization reactions of ERY and THR to ERU proceed via an enediol intermediate at the used reaction conditions, as witnessed by the fact that the C1 position of ERU predominantly was deuterated, if the reaction was conducted in D_2O (Figure S6). The slower enolization of aldotetroses in the formation of ERU, relative to the enolization of GA in the formation of aldotetroses, can be rationalized with the low population of non-cyclic aldehyde forms for aldotetroses (3% for aldotetroses vs 14% for GA at 333 K). On the other hand, the conversion of aldotetroses to hexoses is limited by the decreasing availability of GA upon reaction progress, and by low populations of aldotetrose in its aldehyde form. Due to the higher fraction of GA than tetrose in free aldehyde form, 1,2-ethenediol encounters more C4 aldehyde species than C2 aldehyde species only above 80% conversion of GA to tetroses. Hence, the selectivity towards [2+2] aldol addition appears to sharply decrease above 80% conversion (Figure 7). Overall, cyclization

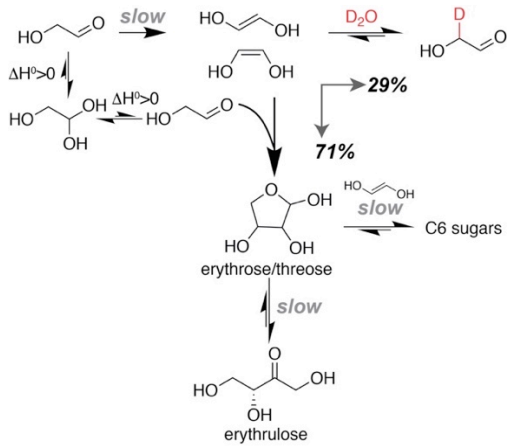

Scheme 2. Schematic overview over reaction mechanisms and kinetics rationalizing the selective formation of kinetically stabilized aldotetroses. Both enolization of the aldotetrose towards ERU, and the competition for aldol addition with the GA enediol are disfavoured by the cyclization of the aldotetroses.

of ERY and THR thus plays a key role in limiting the availability of free aldehyde groups for aldose-ketose-isomerization and for further aldol addition towards C6 sugars.

Conclusion

NMR spectroscopic reaction tracking in conjunction with detailed ex situ analyses shed light on substrate complexity, intermediate formation, and selectivity in the aldol addition of GA over weakly basic AA21 resin. Using deuteration of GA as a reporter reaction, the formation of the 1,2-enediol could be tracked. Formation of the 1,2-enediol in a rate-determining first-order reaction was likely rate-limiting for aldotetrose formation from GA at the concentrations relevant for intensification (mass fractions above 5%), as evident from the parallel emergence of deuterated GA and aldotetroses in NMR reaction tracking. Aldotetroses are kinetically stabilized through cyclization, slowing the conversion to thermodynamically preferred products (ketotetrose and hexoses; Scheme 2). The product distribution reported herein resembles homogeneous basic systems described in the literature. However, heterogeneous systems are typically easier to scale up with simpler separation and purification of products. Finally, we note that Lewis-acid catalysed conversion of GA to tetroses has previously shown a more efficient conversion of GA to the aldotetrose ERU.[2f] Lewis acids are suspected to favour ring opening[17] and cascade reactions (often including hydride shifts)[18] upon coordination to lone pairs at the aldehyde carbonyl group and nearby alcohols. Lewis acids even render carbohydrate enol species detectable by optimized NMR methods[14a, 19] and elicit a more concerted sequence of aldol addition and isomerization steps to the thermodynamically preferred tetrose ERU.[16] We therefore propose that a promising strategy for the production of rare aldotetroses would focus on the use and development of thermally stable basic resins, whose active site structures may be varied to fine-tune the relative preference towards ERY or THR formation.

Experimental Section

Ex situ kinetics

Amberlyst® A21 and D_2O were obtained from Sigma Aldrich, while glycolaldehyde was produced, purified and provided by Haldor Topsøe AS. Batch experiments were conducted in 250 mL glass flasks containing 100 mL demineralized water and specified amounts of glycolaldehyde which was added in its dimer form (per default at 10% w/v) under stirring. Pre-treated Amberlyst® A21 was last added at the desired mass fraction. Batch reactions were incubated in a pre-heated water bath for desired reaction times. Prior to the addition of catalyst and after desired variable reaction times, samples of 1.5 mL volume were collected, sterile-filtered through a 45 μl syringe filter and subjected to analytical HPLC runs.

Product analysis

Analytical HPLC measurements were performed on a Waters 1260 Infinity II LC system equipped with a Biorad Aminex® HPX-87H column and an RI detector. A column temperature of 338 K and 0.004 M H_2SO_4 eluent was used in runs employing a flow rate of 0.6 mL/min and an injection volume of 1 μL. Signal assignments and the respective response factors for quantitative determinations were derived by comparison and calibration relative to analytical HPLC runs on defined masses of commercial reference compounds. Quantitative determinations were compared to qNMR determinations due to the possible presence of impurities in the commercial reference compounds (Figure S7). Determination with HPLC and qNMR quantifications had a coefficient of determination R^2 above 0.9994 for all tetroses. Representative HPLC traces alongside retention times are provided in Figure S8. Yields for tetroses were determined from these quantifications as yield=mass(tetrose)/(mass($GA_{initial}$)). The conversion of glycolaldehyde was determined from the quantifications as conversion=[mass($GA_{initial}$)-mass($GA_{remaining}$)]/(mass($GA_{initial}$)). The selectivity for tetroses was determined from the quantifications as selectivity=mass(tetrose)/[mass($GA_{initial}$)-mass($GA_{remaining}$)].

Thermodynamic equilibrium of aldoses

Reaction mixtures containing erythrose or erythrulose instead of glycolaldehyde substrate were incubated at 323 K for 7 days in the presence of Amberlyst® A21 and post-reaction material was analysed with analytical HPLC determines as described above. The product mixtures derived from erythrose or erythrulose showed a nearly identical distribution of aldoses, with the latter forming the thermodynamically preferred product in thermal equilibrium (approximately 23% threose, 9% erythrose and 68% erythrulose, consistent with distributions determined in literature).

Determination of reaction order with the initial rate method and ex situ analysis

Reaction mixtures were prepared with varying glycolaldehyde and catalyst content, in order to determine the reaction order from ex situ determinations of initial rates with analytical HPLC. Ex situ measurements strongly indicated a first order reaction with respect to both the glycolaldehyde and the catalyst concentration. The first order kinetics with respect to glycolaldehyde was consistent with a rate-determining unimolecular enolization in the rate-determining step.

NMR spectroscopy

All NMR spectra were acquired at 298 K on am 800 MHz Bruker instrument equipped with a TCI CryoProbe. ^1H and ^{13}C assignments for glycolaldehyde species were derived by dissolving 50 mg glycolaldehyde in 500 μl D_2O prior to the acquisition of ^1H-^{13}C HSQC, HMBC and H2BC spectra. The sample was thermally equilibrated at 303 K, 313 K, 323 K and 333 K until signal areas were stable in ^1H NMR spectroscopy, and quantitative ^1H NMR spectra were acquired by summing 16 transients with an inter-scan relaxation delay of 10 s. Mixture analysis and quantitative NMR on the reaction mixture were

conducted by employing 1D ^{13}C NMR with an inter-scan relaxation delay of 30 s for the analysis of protonated ^{13}C sites at natural abundance of ^{13}C relative to $DMSO_2$ as the internal standard.[20] Highly-resolved ^{1}H-^{13}C HSQC spectra[21] were used for the identification and relative quantification of minor species, specifically minor glycolaldehyde and aldotetrose forms as well as hexoses. Populations of threose determined in this way were approximately 37% α-furanose, 54% β-furanose and 9% acyclic species (predominantly hydrate), while populations of erythrose forms were 64% α-furanose, 25% α-furanose and 11% acyclic species.

Amberlyst® A21 catalyzed reactions were followed *in situ* for approximately 24 hours by dissolving 50 mg glycolaldehyde in 500 µl D_2O, adding 20 mg (or 125 mg) Amberlyst® A21 and following the reaction by a pseudo-2D spectrum representing a time series of one-dimensional ^{13}C NMR spectra at 333 K and a time resolution (duration per ^{13}C NMR spectrum) of 7.5 minutes. A reference experiment in the absence of catalyst showed that the glycolaldehyde solution was thermally stable at 333 K (Fig. S4a). A reference experiment in the presence of erythrose and of catalyst showed that erythrose slowly isomerized to erythrulose as the main product at 333 K (Fig. S4b). A reference experiment of a synthetic mixture of erythrose, glycolaldehyde and catalyst showed that erythrose is more slowly converted than the acyclic glycolaldehyde (Fig. S9). All NMR spectra were acquired, processed and integrated with Bruker TopSpin 3.5 or 4.0.6 software. All spectra were processed with ample zero filling in all dimensions. Glycolaldehyde conversion was fitted to first order kinetics in QuantumSoft proFit7.

Acknowledgements

S.M. gratefully acknowledges the Independent Research Fund Denmark (Green transition programme, grant 0217-00277A). 800 MHz NMR spectra NMR spectra were recorded at the NMR Center DTU, supported by the Villum Foundation.

Keywords: glycolaldehyde • tetrose • carbohydrates • kinetics • in situ NMR

[1] C. Chatterjee, F. Pong, A. Sen, *Green Chem.* **2015**, *17*, 40-71.

[2] a) J. D. Lewis, S. Van de Vyver, Y. Román-Leshkov, *Angew. Chem. Int. Ed.* **2015**, *54*, 9835-9838; b) Y. Román-Leshkov, C. J. Barrett, Z. Y. Liu, J. A. Dumesic, *Nature* **2007**, *447*, 982-985; c) S. Van de Vyver, Y. Román-Leshkov, *Angew. Chem. Int. Ed.* **2015**, *54*, 12554-12561; d) M. J. Antal Jr, T. Leesomboon, W. S. Mok, G. N. Richards, *Carbohyd. Res.* **1991**, *217*, 71-85; e) M. J. Antal, W. S. L. Mok, G. N. Richards, *Carbohyd. Res.***1990**, *199*, 91-109; f) S. Tolborg, S. Meier, S. Saravanamurugan, P. Fristrup, E. Taarning, I. Sádaba, *ChemSusChem* **2016**, *9*, 3022; g) R. Zhang, A. Eronen, X. Du, E. Ma, M. Guo, K. Moslova, T. Repo, Green Chem. **2021**, 23, 5481-5486.

[3] a) M. Dusselier, P. Van Wouwe, A. Dewaele, P. A. Jacobs, B. F. Sels, *Science* **2015**, *349*, 78; b) V. Ramaswamy, P. Shah, K. Lazar, A. V. Ramaswamy, *Catal. Surv. sia* **2008**, *12*, 283-309.

[4] a) S. Yamaguchi, T. Matsuo, K. Motokura, Y. Sakamoto, A. Miyaji, T. Baba, *ChemSusChem* **2015**, *8*, 853-860; b) W. H. Faveere, S. Van Praet, B. Vermeeren, K. N. R. Dumoleijn, K. Moonen, E. Taarning, B. F. Sels, *Angew. Chem. Int. Ed.* **2021**, *60*, 12204-12223; c) L. Burroughs, M. E. Vale, J. A. R. Gilks, H. Forintos, C. J. Hayes, P. A. Clarke, *Chem. Comm.* **2010**, *46*, 4776-4778; d) G. Cassone, J. Sponer, J. E. Sponer, F. Pietrucci, A. M. Saitta, F. Saija, *Chem. Comm.* **2018**, *54*, 3211-3214; e) I. V. Delidovich, A. N. Simonov, O. P. Taran, V. N. Parmon, *ChemSusChem* **2014**, *7*, 1833-1846; f) B. M. Kabyemela, T. Adschiri, R. M. Malaluan, K. Arai, H. Ohzeki, *Ind. Eng. Chem. Res.* **1997**, *36*, 5063-5067

[5] a) P. A. Majerski, J. K. Piskorz, D. S. A. G. Radlein, *US7094932B2* **2002**; b) P. Kostetskyy, M. W. Coile, J. M. Terrian, J. W. Collins, K. J. Martin, J. F. Brazdil, L. J. Broadbelt, *J. Anal. Appl. Pyrolysis* **2020**, *149*, 104846; c) C. B. Schandel, M. Høj, C. M. Osmundsen, A. D. Jensen, E. Taarning, *ChemSusChem* **2020**, *13*, 688-692.

[6] a) S. Trigerman, E. Biron, A. H. Weiss, *React. Kinet. Catal. Lett.* **1977**, *6*, 269-274; b) T. Matsumoto, S. Inoue, *J. Chem. Soc. Perkin Trans. I* **1982**, 1975-1979.

[7] a) A. Ricardo, M. A. Carrigan, A. N. Olcott, S. A. Benner, *Science* **2004**, *303*, 196; b) A. N. Simonov, L. G. Matvienko, O. P. Pestunova, V. N. Parmon, N. A. Komandrova, V. A. Denisenko, V. E. Vas'kovskii, *Kinet. Catal.* **2007**, *48*, 550-555; c) J. B. Lambert, S. A. Gurusamy-Thangavelu, K. Ma, *Science* **2010**, *327*, 984; d) H.-J. Kim, A. Ricardo, H. I. Illangkoon, M. J. Kim, M. A. Carrigan, F. Frye, S. A. Benner, *J. Am. Chem. Soc.* **2011**, *133*, 9457-9468.

[8] a) S. Pizzarello, A. L. Weber, *Science* **2004**, *303*, 1151; b) A. Córdova, I. Ibrahem, J. Casas, H. Sundén, M. Engqvist, E. Reyes, *Chem. Eur. J.* **2005**, *11*, 4772-4784; c) A. L. Weber, S. Pizzarello, *Proc. Nat. Acad. Sci. U.S.A.* **2006**, *103*, 12713.

[9] a) M. Dusselier, P. Van Wouwe, S. De Smet, R. De Clercq, L. Verbelen, P. Van Puyvelde, F. E. Du Prez, B. F. Sels, *ACS Catal.* **2013**, *3*, 1786-1800; b) R. De Clercq, M. Dusselier, C. Christiaens, J. Dijkmans, R. I. Iacobescu, Y. Pontikes, B. F. Sels, *ACS Catal.* **2015**, *5*, 5803-5811; c) S. Van de Vyver, C. Odermatt, K. Romero, T. Prasomsri, Y. Román-Leshkov, *ACS Catal.* **2015**, *5*, 972-977.

[10] a) J. Kofoed, J.-L. Reymond, T. Darbre, *Org. Biomol. Chem.* **2005**, *3*, 1850-1855; b) A. N. Simonov, O. P. Pestunova, L. G. Matvienko, V. N. Snytnikov, O. A. Snytnikova, Y. P. Tsentalovich, V. N. Parmon, *Adv. Space Res.* **2007**, *40*, 1634-1640.

[11] M. Fedoroňko, P. Temkovic, J. Königstein, V. Kováčik, I. Tvaroška, *Carbohyd. Res.***1980**, *87*, 35-50.

[12] J. Kua, M. M. Galloway, K. D. Millage, J. E. Avila, D. O. De Haan, *J. Phys. Chem. A* **2013**, *117*, 2997-3008.

[13] A. S. Serianni, J. Pierce, S. G. Huang, R. Barker, *J. Am. Chem. Soc.* **1982**, *104*, 4037-4044.

[14] a) P. R. Jensen, S. Meier, *Chem. Comm.* **2020**, *56*, 6245-6248; b) H. Rasmussen, H. R. Sørensen, A. S. Meyer, *Carbohyd. Res.***2014**, *385*, 45-57.

[15] S. Meier, *Catal. Comm.* **2020**, *135*, 105894.

[16] S. Saravanamurugan, A. Riisager, *Catal. Sci. Technol.* **2014**, *4*, 3186-3190.

[17] H. Zhao, J. E. Holladay, H. Brown, Z. C. Zhang, *Science* **2007**, *316*, 1597.

[18] a) M. S. Holm, S. Saravanamurugan, E. Taarning, *Science* **2010**, *328*, 602; b) Y. Roman-Leshkov, M. Moliner, J. A. Labinger, M. E. Davis, *Angew. Chem. Int. Ed.* **2010**, *49*, 8954-8957.; c) S. G. Elliot, E. Taarning, R. Madsen, S. Meier, *ChemCatChem* **2018**, *10*, 1414-1419.

[19] a) P. R. Jensen, R. K. Knudsen, S. Meier, *ACS Sustain. Chem. Eng.* **2020**, *8*, 12270-12276; b) E. Taarning, I. Sádaba, P. R. Jensen, S. Meier, *ChemSusChem* **2019**, *12*, 5086-5091.

[20] a) S. G. Elliot, S. Tolborg, I. Sadaba, E. Taarning, S. Meier, *ChemSusChem* **2017**, *10*, 2990-2996; b) S. G. Elliot, I. Tosi, A. Riisager, E. Taarning, S. Meier, *Top. Catal.* **2019**.

[21] M. Bøjstrup, B. O. Petersen, S. R. Beeren, O. Hindsgaul, S. Meier, *Anal. Chem.* **2013**, *85*, 8802-8808.

Entry for the Table of Contents

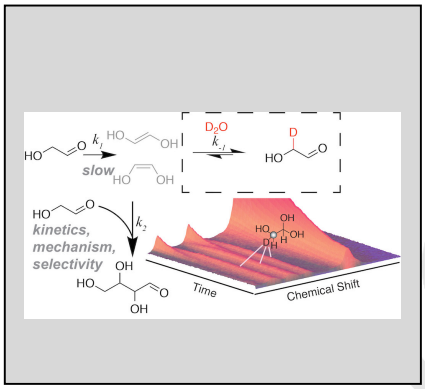

NMR spectroscopic reaction tracking, development of a reporter reaction and ex situ analyses shed light on the details of glycolaldehyde conversion to C4 sugars over weakly basic resin. Formation of a 1,2-enediol in a rate-determining first-order reaction and the kinetic stabilization of the products hint at promising strategies for the production of rare C4 sugars.

Institute and/or researcher Twitter usernames: @DTUKemi @HaldorTopsoe